



FACULTAD DE CIENCIAS  
UNIVERSIDAD DE CANTABRIA

---

**Search for dark matter production in  
association with top quarks in the  
dilepton final state at  $\sqrt{s} = 13$  TeV**

---

A thesis submitted in fulfillment of the requirements for the

**Degree of Doctor of Philosophy**

---

Written by

**Cédric Prieëls**

Under the supervision of

**Jónatan Piedra Gómez  
Pablo Martínez Ruiz del Árbol**

Santander, June 2020



# Abstract



# Resumen



# Acknowledgments





# Acronyms used

<b>SM</b> Standard Model	<b>LNGS</b> Laboratori Nazionali del Gran Sasso
<b>DM</b> Dark Matter	<b>UED</b> Universal Extra Dimensions
<b>LHC</b> Large Hadron Collider	<b>NFW</b> Navarro-Frenk-White
<b>CMS</b> Compact Muon Solenoid	<b>LAT</b> Fermi Large Telescope
<b>ATLAS</b> A Toroidal LHC ApparatuS	<b>IACT</b> Imaging Atmospheric Cherenkov Telescopes
<b>CERN</b> European Council for Nuclear Research	<b>CTA</b> Cherenkov Telescope Array
<b>QFT</b> Quantum Field Theory	<b>AMS</b> Alpha Magnetic Spectrometer
<b>CMB</b> Cosmic Microwave Background	<b>EFT</b> Effective Field Theory
<b>ML</b> Machine Learning	<b>ISR</b> Initial State Radiation
<b>MFV</b> Minimal Flavour Violation	<b>DMWG</b> Dark Matter Working Group
<b>WIMP</b> Weakly Interactive Massive Particle	<b>MET</b> Missing Transverse Energy
<b>PF</b> Particle Flow	<b>VBF</b> Vector Boson Fusion
<b>BSM</b> Beyond the Standard Model	<b>BR</b> Branching Ratio
<b>MACHO</b> Massive Compact Halo Object	<b>LEP</b> Large Electron Positron collider
<b>MSSM</b> Minimal Supersymmetric Standard Model	<b>ALICE</b> A Large Ion Collider Experiment
<b>SI</b> Spin Independent	<b>PS</b> Proton Synchrotron
<b>SD</b> Spin Dependent	<b>SPS</b> Super Proton Synchrotron
<b>CL</b> Confidence Level	<b>PU</b> Pile Up
<b>QCD</b> Quantum Chromodynamics	<b>PV</b> Primary Vertex
<b>ADMX</b> Axion Dark Matter Experiment	<b>ECAL</b> Electromagnetic Calorimeter
<b>CAST</b> CERN Axion Solar Telescope	<b>HCAL</b> Hadronic Calorimeter
<b>IAXO</b> International Axion Observatory	<b>DT</b> Drift tube
	<b>CSC</b> Cathode Strip Chamber
	<b>RPC</b> Resistive Plate Chamber

<b>TIB/TBD</b> Tracker Inner Barrel and Disks	<b>DAQ</b> Data Acquisition System
<b>TOB</b> Tracker Outer Barrel	<b>DQM</b> Data Quality Monitoring
<b>TEC</b> Tracker EndCap	<b>DCS</b> Detector Control System
<b>HO</b> Hadron Outer	<b>WP</b> Working Point
<b>LS</b> Long Shutdown	<b>SC</b> Super Cluster
<b>GEM</b> Gas Electron Multiplier	<b>KF</b> Kalman Filter
<b>L1</b> Level-1 Trigger	<b>GSF</b> Gaussian Sum Filter
<b>HLT</b> High-Level Trigger	<b>MVA</b> Multi-Variate Analysis

# Contents

<b>1</b>	<b>Introduction</b>	<b>1</b>
<b>2</b>	<b>Objects reconstruction</b>	<b>5</b>
2.1	Particle Flow (PF) algorithm . . . . .	5
2.2	Leptons reconstruction . . . . .	7
2.2.1	Muons . . . . .	7
2.2.2	Electrons . . . . .	9
2.2.3	Taus . . . . .	11
2.3	Jets reconstruction . . . . .	11
2.3.1	B-tagging . . . . .	11
2.4	Missing transverse energy . . . . .	11
2.5	Top reconstruction . . . . .	11
<b>3</b>	<b>Data, signals and backgrounds</b>	<b>13</b>
3.1	Data samples . . . . .	13
3.2	Signal samples . . . . .	13
3.3	Background prediction . . . . .	13
3.3.1	The main background: $t\bar{t}$ . . . . .	13
3.3.2	Drell-Yan estimation . . . . .	13
3.3.3	Non prompt contamination . . . . .	13
3.3.4	Smaller backgrounds . . . . .	13
3.3.5	Weights and corrections applied . . . . .	13
<b>4</b>	<b>Event selection</b>	<b>15</b>
4.1	Signal regions . . . . .	15
4.2	Control regions . . . . .	15
4.3	Background-signal discrimination . . . . .	15

4.3.1	Discriminating variables . . . . .	15
4.3.2	Neural network . . . . .	15
<b>5</b>	<b>Results and interpretations</b>	<b>17</b>
5.1	Systematics and uncertainties . . . . .	17
5.2	Results . . . . .	17
<b>6</b>	<b>Conclusions</b>	<b>19</b>
6.1	Future prospects . . . . .	19
	<b>Appendices</b>	<b>21</b>
	<b>Bibliography</b>	<b>25</b>



# Chapter 1

## Introduction

The Standard Model (SM) of particle physics introduced in Section ?? is nowadays the most accepted mathematical model used to describe the elementary particles and three of the four fundamental forces of nature (electromagnetic, weak and strong interactions). This model is quite simple in concept, but has been able to describe most of the phenomena observed in nature so far with an incredible level of precision, and made a lot of predictions that have now been proven to be true, such as the postulate of the Higgs mechanism [1, 2] followed by the discovery of the Higgs boson itself [3, 4] by the Compact Muon Solenoid (CMS) and A Toroidal LHC ApparatuS (ATLAS) experiments analyzing the proton-proton collisions produced by the Large Hadron Collider (LHC) at a center of mass energy  $\sqrt{s} = 13$  TeV, announced at the European Council for Nuclear Research (CERN) on the 4th of July 2012.

However, as accurate as it seems to be, this theory is known to have several shortcomings which require further investigation. Eventual exotic particles which do not fit in the current model could be the sign of new physics and have therefore been extensively searched for over the course of the last decades in order to enhance our understanding of the Universe and all its constituents.

In this context, the first serious Dark Matter (DM) hypothesis was introduced in the 1970s because of gravitational anomalies observed by several astrophysicists, as a way to explain the apparent non-luminous missing mass in the Universe [5]. Indeed, the visible mass in most galaxies appears to be way too low to explain several astrophysical processes, such as the rotation curves of the galaxies [6], which seems to be incompatible with the well established laws of gravitation. Some additional measurements of the gravitational lensing (in the Bullet Cluster, for example [7]) and the anisotropies observed in the Cosmic Microwave Background (CMB) [8] are other evidences for the existence of DM, as explained in Section ??.

As far as we currently know from cosmological measurements, ordinary baryonic matter only constitutes around 5% of the Universe, while DM represents around 26% of the energy density of the Universe (the rest is being considered as dark energy) [9]. Understanding the nature and properties of this new kind of exotic matter is therefore crucial to try and understand the physics in the Universe, with many large experiments around the world currently involved in such searches.

Nowadays, the existence of DM is well established in the physics community, even though it has never been observed directly, since our only evidences so far for its existence come from its large-scale gravitational effects. While its mass, spin, nature and basic properties are still unknown and extensively studied, one of the best DM candidate is the so-called Weakly Interactive Massive Particle (WIMP), predicted to interact both gravitationally and weakly with SM particles. This would allow direct and indirect detection of such candidates, used as the driving process of many of experiments over the last decades, trying to find the hint of a possible interaction between standard baryonic particles and eventual DM particles, or even between several DM particles themselves. Dark matter production through the use of a particle accelerator colliding SM particles together, such as the LHC, is also a possibility, and will be considered as the main channel towards the eventual detection of this exotic matter throughout this work. The production through colliders is actually able to provide constraints on low dark matter masses as well, in a region where both the direct and indirect searches are less efficient, which makes the LHC a perfect tool to study this kind of Beyond the Standard Model (BSM) physics. These searches will be summarized in Section ??.

However, observing DM is still extremely difficult, mainly because it barely interacts with ordinary baryonic matter, except through gravity (we have to assume that it does interact with SM at least weakly for the sake of this work though, as we would not be able to discover it as an individual particle if it were not the case). This means that nowadays, all the experiments searching for DM have only been able to put constraints on the DM particle mass and on the interaction cross sections between the dark and standard sectors. Actually, even if the collisions between protons produced by the LHC do have a sufficient amount of energy to produce this kind of particles, we would not expect them to interact with our detector, making their detection even harder. The eventual presence of such matter has to be inferred from the study of the interaction between SM particles and CMS itself, since a typical DM-like event consists of at least one energetic SM particle produced in association with a large imbalance in the transverse momentum due to the presence of an eventual DM candidate that was able to escape our detection.

In the context of this work, DM is searched for in association with one or two top quarks which play the role of the SM particle allowing us to trigger the event. This is indeed a perfect channel for this kind of searches if we assume that the interaction between the dark and standard sectors respect the principle of Minimal Flavour Violation (MFV), which can be consistently defined independently of the structure of the new physics model [10]. In this case, this interaction should follow the same Higgs-like Yukawa coupling structure as the usual SM baryonic particles, which actually depend on the mass: the heavier the SM particle considered is, the easier it is for it to couple with the dark sector. This makes the top quark, the most massive of all the fundamental particles observed by far, an excellent object to study in this context.

However, this also means that the phenomenology of this quark is mostly driven by its large mass and that it decays before hadronization can occur, usually into a W boson and a bottom quark. The final state of the process we are interested in is then made of some b jets, leptons and/or quarks and is categorized depending on this number of b-tagged jets and on the decay of the W itself. This work will actually be focused on the two leptons final state, also known as the dileptonic channel,

mostly since this channel does not have lots of background processes raising to a similar final state, even though its branching ratio is the smallest, as will be explained in Section ???. Additionally, leptons are by reconstruction much cleaner than jets: their identification and momentum calculation is easier to perform, and the uncertainties associated to these measurements will be smaller.

The LHC has now been running for 10 years, and several similar searches have already been carried out and published in the past by the CMS and ATLAS collaborations, at different center of mass energies. First of all, at 8 TeV, several searches for a pair of top quarks were published by the CMS (in association with DM in the semileptonic [11] and dileptonic [12] final states) and ATLAS collaborations [13]. Then, at 13 TeV, the ATLAS collaboration published on one hand several studies, considering different final states and different luminosities ( $13.3 \text{ fb}^{-1}$  and  $36.1 \text{ fb}^{-1}$ ) [14, 15, 16]. On the other hand, the CMS collaboration published a few extremely important papers for this study [18, 19]. For the first time in 2019, the results obtained by the  $t/\bar{t}$ +DM and  $t\bar{t}$ +DM analyses have also been combined and published using the 2016 data [20]. Our main objective is now to repeat and improve this analysis while considering the full Run II dataset, globally improving the analysis strategy and including the dileptonic final state for the first time in this combination.

After a general introduction about DM in general in Chapter ??, the experimental setup will be detailed in the Chapter ??. This will include a discussion about the LHC itself, along with a complete description of CMS, the detector used to collect the data that will be analyzed throughout this work. This data has been collected during the years 2016, 2017 and 2018 and corresponds to an integrated luminosity of  $\sim 138 \text{ fb}^{-1}$ , collected during the Run II of operation of the LHC and at a center of mass energy  $\sqrt{s} = 13 \text{ TeV}$ . In particular, a particular care will be given to the explanation of the Particle Flow (PF) algorithm, used to reconstruct the different objects used and that will be defined in the Chapter 2, while the estimation of the different backgrounds and the selection of interesting events will be detailed throughout the Chapters 3 and 4.

Distinguishing between the signal we are searching for and backgrounds having a much higher cross-section and kinematically really close, such as the SM  $t\bar{t}$  without production of DM is not a straightforward task (sometimes a production of missing transverse energy due to the presence of physical neutrinos is even obtained). To isolate the signal and to obtain some discrimination between these kind of processes, an algebraic reconstruction of the event and top-notch Machine Learning (ML) techniques are used in this work, in order to train a network of neurons to perform this task. The main objective is to make them learn how to combine the discriminating power of a set of input variables in order to create a single output variable describing the probability of a single event to be classified as signal or background. All this process will be detailed in Section 4.3.

Finally, a statistical interpretation of our data will be performed and different sources of systematic uncertainties will be considered in Chapter 5. This will allow us to set upper limits on the cross section production value of DM particles in our particular channel and for the simplified models considered in this analysis. The conclusions of this work and some additional future prospects will then finally be presented in Chapter 6.





# Chapter 2

## Objects reconstruction

As we just saw, the CMS detector is made out of different layers, each able to convert the interaction of the particle with the detector into electronic signal that can be measured and stored. However, this electronic signal is made out of raw information coming from different kind of sub-systems and an algorithmic strategy then needs to be put in place in order to read all these separate signals and to combine them in order to extract some useful data, such as the number of particles produced by the collision along with their energy, charge and direction. Producing this kind of data is essential for all the analyses later on which usually rely on these kind of objects in order to search for new physics or make precision measurements.

The algorithm able to combine this raw data and to produce useful variables is the so-called Particle Flow (PF) algorithm [89], which will be described in Section 2.1. Then, a particular focus will be given to the definition and reconstruction of different objects of our particular analysis, such as the leptons (Section 2.2), the jets (Section 2.3), the Missing Transverse Energy (MET) (Section 2.4) and the top reconstruction of the different events considered (Section 2.5).

### 2.1 Particle Flow (PF) algorithm

The Particle Flow (PF) is an algorithm whose aim is to combine in the best way possible all the information coming from the different parts of the CMS detector in order to identify and reconstruct all the particles produced by a particular proton-proton collision provided by the LHC. In order to be as efficient as possible, several principles are fundamental: for example, a magnetic field as large as possible is always important, and the tracker needs to be as efficient and small as possible, in order to have the smallest material budget possible in front of the calorimeters, which then needs to have the smallest granularity possible.

Identifying the different particles produced is quite easy, as represented in Figure 2.1. Indeed, the different kind of particles produced are going to interact with different parts of the detector, and combining the information given by the tracker and the rest of the sub-systems therefore allow to unequivocally identify each particle, in a defined order:

- **Muons** are the easiest particles to identify since they are at principle the only particles leaving many hits in the muon chambers on the outside of the detector. Each muon identified is associated to its track in the tracker, where all the hits matching a muon can therefore be removed, leaving less hits available for the clustering algorithm later on, allowing for a more efficient reconstruction of the following objects.
- **Electrons** do have a charge, so they are visible by the tracker and by the Electromagnetic Calorimeter (ECAL), where they are going to produce an electromagnetic shower. Identify electrons is harder than muons though, bascially because of their associated bremsstrahlung emission of photons that need to be attached to the original electrons to avoid any energy double counting. All the tracker hits corresponding to electrons identified are also removed after identification.
- **Charged hadrons** also leave hits in the tracker and some energy deposits in the ECAL, but mostly in the Hadronic Calorimeter (HCAL), so they are easy to identify as well as a third step.
- **Photons** are on the other hand neutral particles, so they do not lave any hit in the tracker. They therefore appear as some energy deposits for which not corresponding tracker track can be associated.
- Finally, **neutral hadrons** can be identified as particles leaving some energy mostly in the HCAL for which no corresponding tracker track has been found as well.

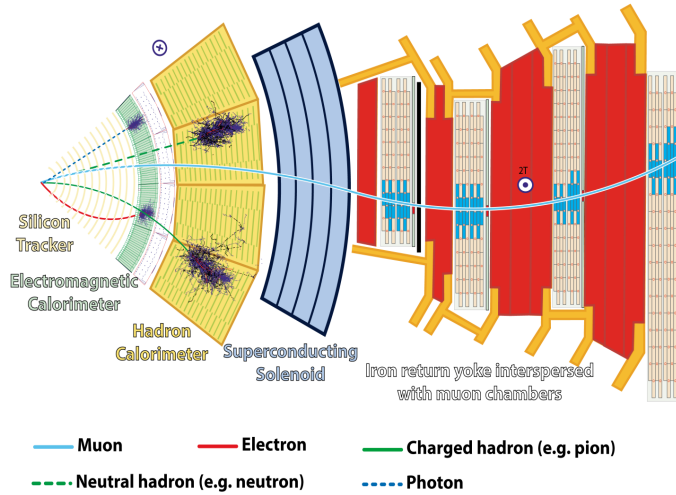


Figure 2.1: Transverse section of CMS, showing the different tracks expected by different kind of particles in the detector.

The efficiency of the PF algorithm for jet identification and reconstruction has been checked using simulation, as shown in Figure 2.2. This study clearly shows that between 95 and 97% of the energy of the PF jet candidates can be reconstructed, compared to a 40-60% reconstruction efficiency using only the calorimeters data, and that this algorithm also leads to a gain in resolution up to a factor 3, depending on the jet  $p_T$ .

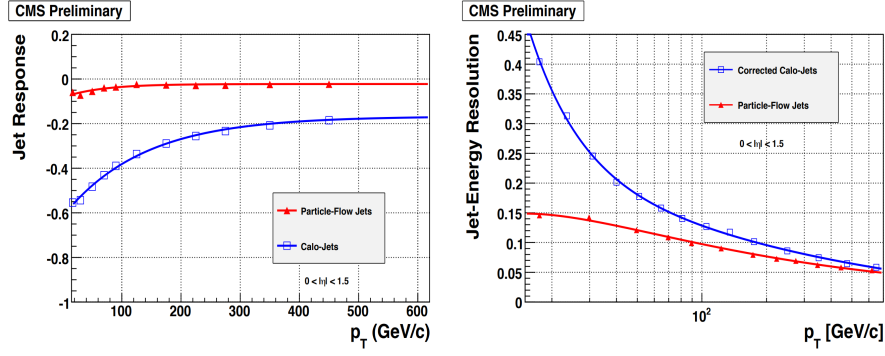


Figure 2.2: Comparison of the jet response (on the left) and jet energy resolution (on the right) for dijets simulated events in the barrel for jets reconstructed using only the calorimeters (in blue) and jet candidates from the PF algorithm (in red) [90].

## 2.2 Leptons reconstruction

Different kind of leptons are typically produced by a proton-proton collision. The muons and the electrons can be quite easily identified, mainly because their lifetime and velocity is high enough, meaning that they are not expected to decay inside the CMS detector, so they can be directly identified. Taus on the other hand are a bit trickier to deal with because they usually decay inside of the beam pipe itself, resulting in a different reconstruction process, as explained in Section 2.2.3.

### 2.2.1 Muons

Muons are the first leptons to be reconstructed by the PF algorithm since, at first order, they are the only particles expected to reach the muon chambers, resulting in their easy identification.

The typical signature of a muon consists in several hits in the silicon tracker associated to a track, since muons do have an electric charge, associated with several hits in the muon chambers, electronic signals coming from the wires and strips of these chambers, due to the gas ionization induced by the passage of these charged particles. Muons only deposit a negligible amount of energy within the two calorimeters since their interaction cross section is quite low for their full range of energies, going from a few hundreds MeV up to a few TeV.

The data coming from the different sub-systems of CMS are then combined and fed into three different PF algorithms, able to reconstruct different kind of muons:

- The **standalone muons** are muons reconstructed using only the hits observed in the muon system, without trying to relate this data to the one observed in the tracker. Basically, the PF algorithm looks in this case at the eventual hits left in the Drift tubes (DTs), Cathode Strip Chambers (CSCs) and Resistive Plate Chambers (RPCs) and tries to reconstruct a segment of

trajectory in each case. These segments are then combined in the best statistical way possible in order to form a candidate track for each muon of the event, constrained additionally by checking the extrapolation of the track to the point on closest approach to the beam line. Candidates reconstructed as standalone muons typically have a worse momentum reconstruction and are more sensitive to cosmic muons contamination.

- The **tracker muons** on the other hand is able to propagate tracker tracks (whose momentum  $p > 2.5$  GeV and  $p_T > 0.5$  GeV) to the muon system itself in order to try and find corresponding segments in the different muon chambers (these tracks are therefore said to be built inside-out). These tracks are particularly efficient for less instrumented regions of the detector and for low  $p_T$  candidates but they are also quite contaminated with fake muons tracks, since a single hit in any of the muon chambers is enough for the candidate to be considered a muon, but hadron shower remnants can quite easily reach the innermost muon station.
- Finally, the **global muons** are built outside-in since they are obtained matching standalone muon tracks with independently reconstructed tracks coming from the tracker itself (of course, in order to avoid any double counting, global muons and tracker muons that share the same tracker track are actually merged into a single candidate). This category of muons presents the advantage of being less sensitive to the muon misidentification rate than tracker muons since it uses the information from more than one muon chamber. The  $p_T$  measurement in this case is also improved (especially at high  $p_T$ ,  $> 200$  GeV) by exploiting the information from both the inner tracker and the muon system.

Using this strategy, about 99% of the muons produced within the geometrical acceptance of the muon system are reconstructed either as global or tracker muons [88], as seen in Figure 2.3.

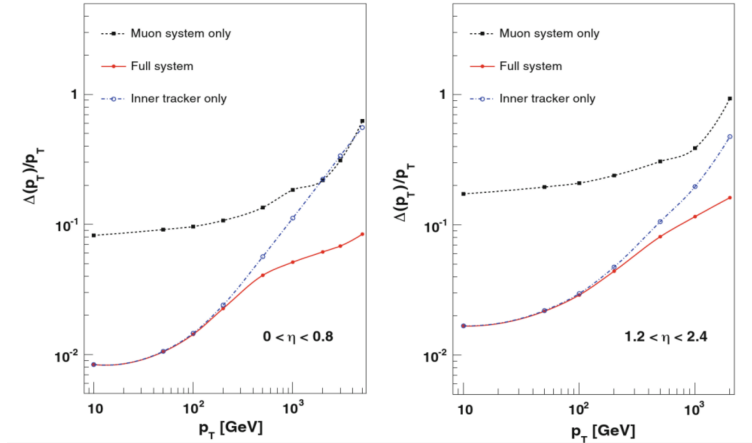


Figure 2.3: Muon  $p_T$  resolution obtained in simulation in the barrel (on the left) and endcap (on the right) for different kind of reconstructed muons [91].

Once reconstructed, candidates are required to pass some selection criteria and are then fed to the actual PF algorithm itself to start the global reconstruction of the event. This selection consists mainly in applying identification and isolation (evaluated relative to its  $p_T$  by summing up the

energy in geometrical cones of radius  $\Delta R = \sqrt{(\Delta\phi)^2 + (\Delta\eta)^2}$  surrounding the muon) criteria in order to enhance the purity of the reconstructed muons. Different Working Points (WPs) can then be defined, from loose to tight, in order to reject more or less contamination from misidentified leptons, keeping in mind that a tighter selection will also have an impact on the efficiency of the selection. The actual selection applied in this particular analysis will be detailed in Chapter 4.

## 2.2.2 Electrons

Electrons are reconstructed by combining the tracker tracks and the several clusters of energy deposited in the ECAL because of the electromagnetic showers appearing due to the interaction between the actual electron and the crystals composing the ECAL. It is usually a bit harder though to reconstruct electrons than muons, mainly because they do interact with the tracker and it is therefore needed to model this interaction to understand the exact behaviour of such particles, since this interaction might be responsible for the emission of secondary photons crashing into the ECAL but not coming from the Primary Vertex (PV). In fact, it is estimated that in CMS, depending on its pseudorapidity, between 33% and 86% of the energy of an electron is actually radiated before it reaches the ECAL [92].

The first step for the identification and measurement of the properties of the electrons consist in clustering all the energy deposited in the ECAL, and this is not an easy because electrons usually deposit their energy into several different crystals because of the electromagnetic shower effect discussed in Section ???. In order to measure precisely the energy of an electron, all the photons emitted by bremsstrahlung before reaching the ECAL (usually, along the  $\phi$  axis because of the deviation implied by the solenoid) need to be collected and associated to the correct electron of the event.

The actual PF reconstruction of electrons is performed in different steps:

- A **clustering algorithm** quite powerful is first of all defining the so-called Super Cluster (SC). Its goal is to reconstruct the particle showers individually by first of all identifying a seed crystal for the cluster, defined as the crystal collecting the most energy.

The algorithm then searches for eventual crystals around this seed whose energy detected would be superior to  $2\sigma$  of the electronic noise and matching some quality criteria ( $E_{\text{seed}} > 230$  MeV in the barrel,  $E_{\text{seed}} > 600$  MeV and  $E_{\text{seed}}^T > 150$  MeV in the endcaps).

The excited contiguous crystals are then grouped into clusters, themselves considered for the final global cluster, the SC, if their energy is higher than another given threshold ( $E_{\text{cluster}} > 350$  MeV in the barrel,  $E_{\text{cluster}}^T > 1$  GeV in the endcaps) [92]. The SC energy is then given by the sum of the energies of all its constituent clusters, while its position is calculated as the energy-weighted mean of the positions of the different clusters.

- Once the SC identified, **electron tracker tracks** are reconstructed, using a procedure a bit different than the usual Kalman Filter (KF) reconstruction method for all the tracks of the silicon tracker [93] because of the large radiative losses for electrons in the tracker material.

This procedure being very time consuming, a good identification of potential electron seeds has to be performed as the method efficiency greatly relies on this first identification. Two different strategies can be used to perform this seeding: first of all, the ECAL-based seeding relies on the information obtained for the SC energy and position in order to estimate the electron trajectory to find compatible hits in the tracker. This can be done knowing that the electron or positron is moving according to an helix in the magnetic field of the detector. The other way to proceed is the tracker-based seeding, based on tracks reconstructed using the usual algorithm and looking for matches within the possible reconstructed SC. Usually, the electron seeds found using the two algorithms are then combined.

Once the seeds identified, the identification of tracks itself can begin. First of all, the gathering of compatible hits from the different seeds is done using the combinatorial KF algorithm, and when compatible hits have been found, possible tracks are constructed based on these hits, with a  $\chi^2$  penalty applied to eventual track candidates with one missing hit. The compatibility matching between the predicted and found hits is usually chosen to be quite loose in order to maintain a good efficiency even in case of bremsstrahlung emission.

Finally, once the hits are collected, a Gaussian Sum Filter (GSF) fit is performed to estimate the different track parameters. A mix of Gaussian distributions is used in this case to approximate the loss in each layer, associating a different weight to each distribution.

- The final step consists in **merging the GSF track and the ECAL SCs** previously built. This step is also designed to preserve the highest efficiency possible while keeping the misidentification probability low, and uses different track-cluster association criteria depending on the seeding used (either cuts on the angles between the SC and the and the GSF track in the ECAL-seeding case, or a complete Multi-Variate Analysis (MVA) using track observables, electron PF cluster observables and relations between the two for the tracker-seeding). Ambiguities concerning eventual single electron seeds which can often lead to several reconstructed tracks are also resolved at this stage.

This complete electron workflow explained here in a simplified way can be summarized in Figure 2.4.

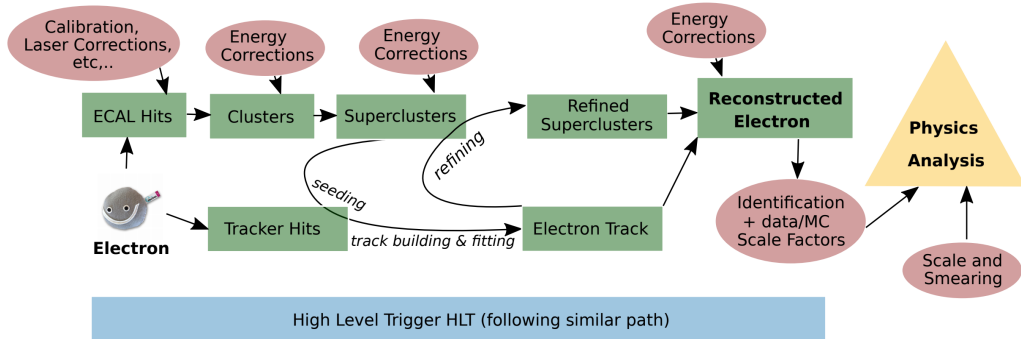


Figure 2.4: Schematic representation of the full electron reconstruction workflow in CMS [94].

## **2.3 Jets reconstruction**

### **2.3.1 B-tagging**

## **2.4 Missing transverse energy**

## **2.5 Top reconstruction**





## Chapter 3

# Data, signals and backgrounds

### 3.1 Data samples

### 3.2 Signal samples

### 3.3 Background prediction

#### 3.3.1 The main background: $t\bar{t}$

#### 3.3.2 Drell-Yan estimation

#### 3.3.3 Non prompt contamination

#### 3.3.4 Smaller backgrounds

#### 3.3.5 Weights and corrections applied



## Chapter 4

# Event selection

### 4.1 Signal regions

### 4.2 Control regions

### 4.3 Background-signal discrimination

#### 4.3.1 Discriminating variables

#### 4.3.2 Neural network



## Chapter 5

# Results and interpretations

### 5.1 Systematics and uncertainties

### 5.2 Results



## Chapter 6

# Conclusions

### 6.1 Future prospects





# Appendices



# List of figures

2.1	Transverse section of CMS, showing the different tracks expected by different kind of particles in the detector. . . . .	6
2.2	Comparison of the jet response (on the left) and jet energy resolution (on the right) for dijets simulated events in the barrel for jets reconstructed using only the calorimeters (in blue) and jet candidates from the PF algorithm (in red) [90]. . . . .	7
2.3	Muon $p_T$ resolution obtained in simulation in the barrel (on the left) and endcap (on the right) for different kind of reconstructed muons [91]. . . . .	8
2.4	Schematic representation of the full electron reconstruction workflow in CMS [94]. .	10



# List of tables



# Bibliography

- [1] F. Englert and R. Brout, "Broken symmetry and the mass of gauge vector mesons", Phys. Rev. Lett. 13, pp. 321-323, 1964
- [2] P. W. Higgs, "Broken symmetries and the masses of gauge bosons", Phys. Rev. Lett. 13, pp. 508-509, 1964
- [3] S. Chatrchyan et al., "Observation of a new boson at a mass of 125 GeV with the CMS experiment at the LHC", Phys. Lett. B716, pp. 30-61, 2012 [arXiv: 1207.7235]
- [4] G. Aad et al., "Observation of a new particle in the search for the Standard Model Higgs boson with the ATLAS detector at the LHC", Phys. Lett. B716, pp. 1-29, 2012 [arXiv: 1207.7214]
- [5] V.C. Rubin, W.K. Ford and N. Thonnard, "Rotational properties of 21 SC galaxies with a large range of luminosities and radii, from NGC 4605 (R=4kpc) to UGC 2885 (R=122kpc)", Astrophysical Journal 238, pp. 471-487, 1980
- [6] K.G. Begeman, A.H. Broeils and R.H. Sanders, "Extended rotation curves of spiral galaxies - Dark haloes and modified dynamics", Monthly Notices of the Royal Astronomical Society, vol. 249, issue 3, ISSN 0035-8711, 1991
- [7] A. Robertson, R. Massey and V. EkCMBTemperaturee, "What does the Bullet Cluster tell us about self-interacting dark matter?", Monthly Notices of the Royal Astronomical Society, vol. 465, issue 1, 2017 [arXiv: 1605.04307]
- [8] J.B. Mu?oz, C. Dvorkin and A. Loeb, "21-cm Fluctuations from Charged Dark Matter", Phys. Rev. Lett. 121, 121301 (2018) [arXiv: 1804.01092]
- [9] A. Natarajan, "A closer look at CMB constraints on WIMP dark matter", Phys. Rev. D85, 2012 [arXiv:1201.3939 ]
- [10] G. D'Ambrosio G.F. Giudice, G. Isidori and A. Strumia, "Minimal Flavour Violation: an effective field theory approach", Nucl.Phys. 645, pp 155-187, 2002 [arXiv:0207.036 ]
- [11] CMS Collaboration, "Search for the production of dark matter in association with top-quark pairs in the single-lepton final state in proton-proton collisions at  $\sqrt{s} = 8$  TeV", JHEP, vol. 6 121, 2015
- [12] CMS Collaboration,, "Search for the Production of Dark Matter in Association with Top Quark Pairs in the Di-lepton Final State in pp collisions at  $\sqrt{s} = 8$  TeV", CMS-PAS-B2G-13-004, 2014



- [13] "Search for dark matter in events with heavy quarks and missing transverse momentum in pp collisions with the ATLAS detector", Eur. Phys. J. C (2015) 75:92
- [14] ATLAS Collaboration, Search for the Supersymmetric Partner of the Top Quark in the Jets+Emiss Final State at  $\sqrt{s} = 13$  TeV", ATLAS-CONF-2016-077
- [15] ATLAS Collaboration, "Search for top squarks in final states with one isolated lepton, jets, and missing transverse momentum in  $\sqrt{s} = 13$  TeV pp collisions with the ATLAS detector", ATLAS-CONF-2016-050, 2016
- [16] ATLAS Collaboration, "Search for direct top squark pair production and dark matter production in final states with two leptons in  $\sqrt{s} = 13$  TeV pp collisions using 13.3 fb<sup>-1</sup> of ATLAS data", ATLAS-CONF-2016-076, 2016
- [17] ATLAS Collaboration, "Search for dark matter produced in association with bottom or top quarks in  $\sqrt{s} = 13$  TeV pp collisions with the ATLAS detector", Eur. Phys. J. C 78 (2018) 18 [arXiv: 1710.11412]
- [18] CMS Collaboration, Search for dark matter produced in association with heavy-flavor quark pairs in proton-proton collisions at  $\sqrt{s} = 13$  TeV", Eur. Phys. J. C (2017) 77: 845
- [19] CMS Collaboration, "Search for dark matter particles produced in association with a top quark pair at  $\sqrt{s} = 13$  TeV", Phys. Rev. Lett. 122, 011803 (2019) [arXiv: 1807.06522]
- [20] CMS Collaboration, "Search for dark matter produced in association with a single top quark or a top quark pair in proton-proton collisions at  $\sqrt{s} = 13$  TeV", JHEP, vol. 03 141, 2019 [arXiv: 1901.01553]
- [21] S. Manzoni, "The Standard Model and the Higgs Boson", Physics with Photons Using the ATLAS Run 2 Data, Springer Theses, 2019
- [22] A.B. Balantekin, A. Gouvea and B.Kayser, "Addressing the Majorana vs. Dirac Question with Neutrino Decays", FERMILAB-PUB-18-418-T, NUHEP-TH/18-09 [arXiv: 1808.10518]
- [23] J. Woithe, G.J. Wiener and F. Van der Vecken, "Let's have a coffee with the Standard Model of particle physics!", Physics education 52, number 3, 2017
- [24] F. Zwicky, "Die Rotverschiebung von extragalaktischen Nebeln", Helvetica Physica Acta , vol. 6, pp. 110-127, 1933
- [25] S. Van den Bergh, Phys Rev D "The early history of dark matter", Dominion Astrophysical Observatory, 1999
- [26] V.C. Rubin, W.K. Ford, "Rotation of the Andromeda Nebula from a Spectroscopic Survey of Emission Regions", Astrophysical Journal 159, p. 379, 1970
- [27] A. A. Penzias, R.W. Wilson, "A Measurement of Excess Antenna Temperature at 4080 Mc/s", Astrophysical Journal 142, pp. 419-421

- [28] D.J. Fixsen, "The temperature of the cosmic microwave background", *Astrophysical Journal*, 2009
- [29] Planck Collaboration, "Planck 2018 results. I. Overview and the cosmological legacy of Planck", 2018 [arXiv: 1807.06205]
- [30] R. Tojeiro, "Understanding the Cosmic Microwave Background Temperature Power Spectrum", 2006
- [31] Planck Collaboration, "Planck 2018 results. VI. Cosmological parameters", 2018 [arXiv: 1807.06209]
- [32] "Astrophysical Constants and Parameters", 2019
- [33] D. Clowe et al., "A Direct Empirical Proof of the Existence of Dark Matter", *Astrophysical Journal Letters* 648, 2006
- [34] K.R. Dienes, J. Fennick, J. Kumar, B. Thomas "Dynamical Dark Matter from Thermal Freeze-Out", *Phys. Rev. D* 97, 063522 (2018) [arXiv: 1712.09919]
- [35] C.S. Frenk, S.D.M. White, "Dark matter and cosmic structure", *Annalen der Physik*, p. 22 , 2012 [arXiv: 1210.0544]
- [36] R. Kirk, "Dark matter genesis"
- [37] M. Drewes et al., "A White Paper on keV Sterile Neutrino Dark Matter", 2016 [arXiv: 1602.04816]
- [38] C. Alcock et al., "The MACHO Project: Microlensing Results from 5.7 Years of LMC Observations", *Astrophys.J.* 542 (2000) 281-307
- [39] P. Tisserand et al., "Limits on the Macho content of the Galactic Halo from the EROS-2 Survey of the Magellanic Clouds", *A & A* 469, pp. 387-404 (2007)
- [40] EROS and MACHO collaborations, "EROS and MACHO Combined Limits on Planetary Mass Dark Matter in the Galactic Halo", 1998
- [41] Particle Data Group, "Neutrino Cross Section Measurements", PDG 2019
- [42] K. McFarland, "Neutrino Interactions", 2008 [arXiv: 0804.3899]
- [43] E. Morgante, "Aspects of WIMP Dark Matter Searches at Colliders and Other Probes", Springer theses, 2016
- [44] F. Couchot et al., "Cosmological constraints on the neutrino mass including systematic uncertainties", *A & A* 606, A104 (2017)
- [45] E. Bulbul et al., "Detection of An Unidentified Emission Line in the Stacked X-ray spectrum of Galaxy Clusters", 2014 [arXiv: 1402.2301]
- [46] A. Boyarsky et al., "An unidentified line in X-ray spectra of the Andromeda galaxy and Perseus galaxy cluster", *Phys. Rev. Lett.* 113, 251301 (2014) [arXiv: 1402.4119]

- [47] A. Boyarsky et al., "Checking the dark matter origin of 3.53 keV line with the Milky Way center", Phys. Rev. Lett. 115, 161301 (2015) [arXiv: 1408.2503]
- [48] T. Jeltema and S. Profumo, "Deep XMM Observations of Draco rule out at the 99% Confidence Level a Dark Matter Decay Origin for the 3.5 keV Line", 2015 [arXiv: 1512.01239]
- [49] D. Wu, "A Brief Introduction to the Strong CP Problem", Superconducting Super Collider Laboratory, 1991
- [50] R.D. Peccei, H.R. Quinn, "CP Conservation in the Presence of Pseudoparticles", Phys. Rev. Lett. 38, 1440, 1977
- [51] P.W. Graham et al., "Experimental Searches for the Axion and Axion-like Particles", Annual Review of Nuclear and Particle Science 65, 2015 [arXiv: 1602.00039]
- [52] CAST collaboration, "New CAST limit on the axion-photon interaction", Nature Physics 13, pp. 584-590 (2017)
- [53] B. Penning, "The Pursuit of Dark Matter at Colliders - An Overview", 2017 [arXiv: 1712.01391]
- [54] M. Schumann, "Direct Detection of WIMP Dark Matter: Concepts and Status", J. Phys. G46 (2019) no.10, 103003 [arXiv: 1903.03026]
- [55] S.C. Martin et al., "The RAVE survey: constraining the local Galactic escape speed", Mon.Not.Roy.Astron.Soc.379:755-772, 2007
- [56] K. Freese, M. Lisanti, C. Savage, "Annual Modulation of Dark Matter: A Review", [arXiv: 1209.3339v3]
- [57] T.M. Undagoitia and L. Rauch, "Dark matter direct-detection experiments", J. Phys. G43 (2016) no.1, 013001 [arXiv: 1509.08767]
- [58] R. Bernabei et al., "First results from DAMA/LIBRA and the combined results with DAMA/NaI", Eur.Phys.J.C56:333-355, 2008 [arXiv: 0804.2741]
- [59] J.M. Gaskins, "A review of indirect searches for particle dark matter", Contemporary Physics, 2016 [arXiv: 1604.00014]
- [60] F.S. Queiroz, "Dark Matter Overview: Collider, Direct and Indirect Detection Searches", Max-Planck Institute of Physics
- [61] LAT collaboration, "Constraints on Dark Matter Annihilation in Clusters of Galaxies with the Fermi Large Area Telescope", JCAP 05(2010)025 [arXiv: 1002.2239]
- [62] A.A. Moiseev et al., "Dark Matter Search Perspectives with GAMMA-400", 2013 [arXiv: 1307.2345]
- [63] L. Covi et al., "Neutrino Signals from Dark Matter Decay", JCAP 1004:017, 2010 [arXiv: 0912.3521]

- [64] B. Lu and H. Zong, "Limits on the Dark Matter from AMS-02 antiproton and positron fraction data", Phys. Rev. D 93, 103517 (2016) [arXiv: 1510.04032]
- [65] J. Abdallah et al., "Simplified Models for Dark Matter Searches at the LHC", Phys. Dark Univ. 9-10 (2015) 8-23 [arXiv: 1506.03116]
- [66] H. An, L. Wang, H. Zhang, "Dark matter with t-channel mediator: a simple step beyond contact interaction", Phys. Rev. D 89, 115014 (2014) [arXiv: 1308.0592]
- [67] ATLAS Collaboration, "Search for dark matter and other new phenomena in events with an energetic jet and large missing transverse momentum using the ATLAS detector", JHEP 01 (2018) 126 [arXiv: 1711.03301]
- [68] CMS Collaboration, "Search for new physics in the monophoton final state in proton-proton collisions at  $\sqrt{s} = 13$  TeV", J. High Energy Phys. 10 (2017) 073 [arXiv: 1706.03794]
- [69] CMS Collaboration, "Search for dark matter produced with an energetic jet or a hadronically decaying W or Z boson at  $\sqrt{s} = 13$  TeV", JHEP 07 (2017) 014 [arXiv: 1703.01651]
- [70] CMS Collaboration, "Search for new physics in final states with an energetic jet or a hadronically decaying W or Z boson and transverse momentum imbalance at  $\sqrt{s} = 13$  TeV", Phys. Rev. D 97, 092005 (2018) [arXiv: 1712.02345]
- [71] ATLAS Collaboration, "Search for dark matter in association with a Higgs boson decaying to two photons at  $\sqrt{s} = 13$  TeV with the ATLAS detector", Phys. Rev. D 96 (2017) 112004 [arXiv: 1706.03948]
- [72] CMS Collaboration, "Search for associated production of dark matter with a Higgs boson decaying to  $b\bar{b}$  or  $\gamma\gamma$  at  $\sqrt{s} = 13$  TeV", JHEP 10 (2017) 180 [arXiv: 1703.05236]
- [73] Atlas Collaboration, "Search for new phenomena in dijet events using 37 fb<sup>-1</sup> of pp collision data collected at  $\sqrt{s} = 13$  TeV with the ATLAS detector", Phys. Rev. D 96, 052004 (2017) [arXiv: 1703.09127]
- [74] CMS Collaboration, "Search for narrow and broad dijet resonances in proton-proton collisions at  $\sqrt{s} = 13$  TeV and constraints on dark matter mediators and other new particles", JHEP 08 (2018) 130 [arXiv: 1806.00843]
- [75] C. Munoz, "Models of Supersymmetry for Dark Matter", FTUAM 17/2, IFT-UAM/CSIC-17-005, 2017 [arXiv: 1701.05259]
- [76] CMS Collaboration, "Searches for invisible decays of the Higgs boson in pp collisions at  $\sqrt{s} = 7, 8$ , and 13 TeV", JHEP 02 (2017) 135 [arXiv: 1610.09218]
- [77] J. Alimena et al., "Searching for long-lived particles beyond the Standard Model at the Large Hadron Collider", 2019 [arXiv: 1903.04497]
- [78] A. Albert et al., "Recommendations of the LHC Dark Matter Working Group: Comparing LHC searches for heavy mediators of dark matter production in visible and invisible decay channels", 2017 [arXiv: 1703.05703]

- [79] M. Tanabashi et al., Particle Data Group, Phys. Rev. D98, 030001 (2018)
- [80] R. Schicker, "The ALICE detector at LHC", 2005
- [81] LHCb Collaboration, "LHCb Detector Performance", Int. J. Mod. Phys. A 30, 1530022 (2015) [arXiv: 1412.6352]
- [82] E. Gschwendtner, "AWAKE, A Particle-driven Plasma Wakefield Acceleration Experiment", CERN Yellow Report CERN 2016-001, pp.271-288 [arXiv: 1705.10573]
- [83] M. Thomson, "Modern Particle Physics", Cambridge University Press, 2013
- [84] G. Apollinari et al., "High Luminosity Large Hadron Collider HL-LHC", CERN Yellow Report CERN-2015-005, pp.1-19 [arXiv: 1705.08830]
- [85] CMS Collaboration, "The CMS experiment at the CERN LHC", JINST 3 (2008) S08004
- [86] CMS Collaboration, "Precision measurement of the structure of the CMS inner tracking system using nuclear interactions", JINST 13 (2018) P10034 [arXiv: 1807.03289]
- [87] M.S. Kim, "CMS reconstruction improvement for the muon tracking by the RPC chambers", 2013 JINST 8 T03001 [arXiv: 1209.2646]
- [88] CMS Collaboration, "Performance of the CMS muon detector and muon reconstruction with proton-proton collisions at  $\sqrt{s} = 13$  TeV", JINST 13 (2018) P06015 [arXiv: 1804.04528]
- [89] CMS Collaboration, "Particle-Flow Event Reconstruction in CMS and Performance for Jets, Taus, and MET", CMS-PAS-PFT-09-001, 2009
- [90] F. Beaudette, "The CMS Particle Flow Algorithm", 2014 [arXiv: 1401.8155]
- [91] V. Knunz, "Measurement of Quarkonium Polarization to Probe QCD at the LHC", Springer theses, 2015
- [92] CMS Collaboration, "Performance of electron reconstruction and selection with the CMS detector in proton-proton collisions at  $\sqrt{s} = 8$  TeV", JINST 10 (2015) P06005 [arXiv: 1502.02701]
- [93] CMS Collaboration, "Description and performance of track and primary-vertex reconstruction with the CMS tracker", JINST 9 (2014) P10009 [arXiv: 1405.6569]
- [94] J. Rembser, "CMS Electron and Photon Performance at 13 TeV", J. Phys. Conf. Ser. 1162 012008, 2019